

Supporting information

Silicon quantum dots promote radish resistance to root herbivores without impairing rhizosphere microenvironment health

Ningke Fan ^a, Chunjie Zhao ^a, Zihao Chang ^a, Le Yue ^a, Feng He ^a, Zhenggao Xiao ^{a, *},

Zhenyu Wang ^a

^a Institute of Environmental Processes and Pollution Control, School of Environmental
and Civil Engineering, Jiangnan University, Wuxi, 214122, China

* Corresponding author:

E-mail address: zhenggao.xiao@jiangnan.edu.cn (Z. Xiao)

Number of Pages: 23

Number of Texts: 9

Number of Tables: 5

Number of Figures: 9

Text S1. Synthesis and characterization of Si QDs

Silicon quantum dots (Si QDs) was synthesized by one-step method according to a previous research.¹ 2.3 g sodium ascorbate was dissolved with 8.0 mL ultrapure water, and then 2.0 mL N-[3-(Trimethoxysilyl)propyl]ethylenediamine (Sigma Aldrich) was mixed with the above sodium ascorbate solution in 80 °C water bath. After 8 h of stirring, the overplus reactants were removed with a dialysis bag (1000Da, molecular weight cutoff) for about 48 h. Finally, the solid Si QDs were obtained by freeze-drying. The shape and size of Si QDs were observed by transmission electron microscopy (TEM, JEM–2100, Hitachi, Japan), and fluorescence spectra were measured with a fluorescence spectrophotometer (F–7000, Hitachi, Japan). The surface functional groups of Si QDs were characterized by Fourier transform infrared spectroscopy (FT–IR, Tensor 27, Bruker Optics, Germany). The dissolution rate of Si QDs was determined by silicomolybdic acid (SMA) spectrophotometric assay (Details in Text S2).

Text S2. Determination of the dissolution rate of Si QDs

The dissolution rate of Si QDs is expressed using the content of silicic acid in the solution.² First, we prepared 50 mg/L Si QDs suspension of two different compositions: (1) deionized water and (2) soil solution (soil: deionized water = 1: 2.5). After sonicating for 30 minutes, these suspensions were placed under constant stir at 100 rpm using temperature controlled shaking incubator (Shanghai Zhichu Instrument Co., Ltd., China) held at 25 °C and aliquots were sampled at specific intervals (0h, 1 day, 5 days, 10 days, 15 days, 25days and 30 days). Subsequently, we used silicomolybdic acid (SMA) spectrophotometric assay to determine content of silicic acid.² In a 2 mL centrifuge tube, 0.1 mL of the suspension, and 0.15 mL of the solution A were mixed. After 10 minutes, 0.75 mL of the solution B was added to the mixture. After 2 hours of incubation, the absorbance of the reaction solution was detected at 810 nm with a multifunctional microplate reader (Varioskan Lux, Thermo Scientific, Finland). The silicic acid concentration was calculated by comparison of the absorbance of the sample mixtures with those of the diluted silicon standard solutions (GSB04-1752-2004(a), China). The assay solution A was prepared by adding 2 g of ammonium molybdate

tetrahydrate and 6 mL of concentrated hydrochloric acid in deionized water at a total volume of 100 mL. The solution B was prepared by dissolving 2 g of oxalic acid, 0.667 g of 4-methylaminophenol sulphate, 0.4 g of anhydrous sodium sulfite, and 10 mL of concentrated sulfuric acid into deionized water at a total volume of 100 mL.

Text S3 Measurement of rhizosphere soil silicic acid content

According to the method of Ma et al. (2021)³, we first extracted soil silicic acid. 0.1 g of air-dried soil sample and 1 g of ultrapure water were added into a 2 mL centrifuge tube, shaken for 5 h and centrifuged at 6000 r/ min for 30 min. The soil solution was filtered with a 0.45 µm membrane. Subsequently, SMA spectrophotometric assay to determinate soil silicic acid content,² as described in Text S2.

Text S4. Measurement of taproot MDA and antioxidant enzyme activities

Taproot Malondialdehyde (MDA) was estimated based on Ma et al. (2017)⁴. Briefly, 100 mg of radish root were ground into powder with liquid nitrogen and added 1.5 mL of pre-cooled 0.1% trichloroacetic acid (TCA). After centrifuging at 4 °C, 10,000 rpm for 10min, the supernatant (0.25 mL) reacted with 0.5 mL of 20% TCA and 0.5 mL of 0.5% thiobarbituric acid (TBA) at 95 °C for 30 min. Subsequently, the mixture was cooled down on ice before measuring absorbance at 450 nm, 532 nm and 600 nm with a multifunctional microplate reader (Varioskan Lux, Thermo Scientific, Finland). MDA content was determined using the following equation: $C_{MDA}(\mu\text{mol/L}) = 6.45 * (\text{Absorbance}_{532} - \text{Absorbance}_{600}) - 0.56 * \text{Absorbance}_{450}$.

The activity of superoxide dismutase (SOD), peroxidase (POD) and catalase (CAT) in radish roots were analyzed according to the methods of Luo et al. (2021)⁵ with slight modification. Firstly, 100 mg radish taproots were homogenized in 1 mL 50 mM phosphate buffer solution (pH 7.8) under ice bath, and then centrifuged (12000 rpm, 4°C) for 30 min. The supernatant was used as the crude enzyme for activity analysis of SOD, POD and CAT.

For SOD activity, the crude enzyme was mixed with L-methionine, nitroblue tetrazole, riboflavin, and EDTA-Na₂. The mixture was exposed under a fluorescent tube lamp for 20 min, and then determined by a multifunctional microplate at 560 nm. SOD

activity takes the amount of enzyme required to inhibit NBT photoreduction by 50% as one unit of SOD.

For POD activity, the crude enzyme was mixed with 200 mM phosphate buffer solution (pH 6.0) containing guaiacol solution and 30% H₂O₂, the mixtures were immediately measured in the wavelength of 470 nm for 2min each 30s by a multifunctional microplate reader. The increase in OD value of 0.01 per minute was considered as one unit of POD.

For CAT activity, the absorbance of 200 μ L of the reaction mixture (15 mM phosphate buffer (pH 7.0), 0.05% H₂O₂, and 6.67 μ L enzyme extracts) was recorded for 3 min at 240 nm. The reduction of 0.01 of OD value per min was used as one unit of CAT.

Text S5. Determination of Si in soils and taproots

Si in soils and taproots were extracted by microwave digestion and determined by inductively coupled plasma mass spectrometry (ICP–MS, Thermo Fisher, Germany) following our previous study.⁶ Briefly, the 10 mg dried soil sample and 20 mg dried radish taproots were mixed with 3 mL ultrapure water (Milli Q) and 3 mL HNO₃, and digested by a microwave digestion instrument (instrument parameters: 1600 W, 190 °C, Mars 6, USA). Then, the liquid was filtered through a 0.22 μ m membrane, diluted to 100 mL with ultrapure water, and stored at 4 °C for ICP/MS analysis. In order to evaluate the precision and accuracy of the methods, a standard reference material (bush branches and leaves, GBW07602) was also analyzed by the same procedure. Germanium (10 μ g/mL) was used as an internal standard to calibrate the instrument signal drift and matrix suppression. The calibration curve for Si element was obtained by standard addition method, and linearity range and equation, detection limit, and spike recovery were shown in Table S1.

Text S6. Measurement of taproot lignin content

Taproot lignin of radish was measured according our previous study.⁷ Specifically, 100 mg of fresh radish taproots were ground to powder under liquid nitrogen and transferred to 2 mL centrifuge tubes, which, were added with 1.5 mL 95% ethanol, centrifuged, removed the supernatant, and repeated three times. After centrifugation,

the sediment was collected, air dried, and added with 0.2 ml 25% acetyl bromide (acetyl bromide: ice acetic acid = 25:75, v/v) solution, placed in a 70 °C water bath for 30 min, and mixed it upside down every 10 min to ensure that full immersion of the precipitate with the solvent. The reaction was terminated by adding 0.16 mL 2 M NaOH. Next, 2 mL ice acetic acid and 0.04 mL hydroxylamine hydrochloride (521.175 g/L) were added to the samples, well shaken, and centrifuged at a speed of 1000 rpm for 10 min. Finally, 0.1 mL of the supernatant was taken and diluted by adding 2.0 mL ice acetic acid. The absorbance of the reaction solution was detected at 280 nm with a multifunctional microplate reader (Varioskan Lux, Thermo Scientific, Finland).

Text S7. UHPLC-MS/MS for determination of phytohormones

Briefly, 100 mg of radish taproot tissues were ground in liquid nitrogen and added with 1 mL ethyl acetate, including 10 µg/mL butylated hydroxytoluene. After vortexing for 15 min, the samples were ultrasonically extracted in ice for 15 min. After centrifugation (4 °C, 12,000 rpm) for 10 min, the supernatants were transferred into a new tube and freeze-dried. The residual was re-dissolved in 200 µL 70% ethanol (v/v). A 10 µL aliquot of extract solution was then directly injected into a UHPLC-MS/MS system (Vanquish Flex, Thermofisher Scientific, Germany) with a 2.1 × 100 mm × 1.8 µm C18 column (Acquity HSS T3, Waters, USA) coupled to Q-Exactive Plus mass spectrometer (Thermo Fisher Scientific, USA). The UHPLC-MS/MS system was operated at a flow rate of 0.35 mL/min. A mobile phase composed of solvent A (0.01% formic acid in water, v/v) and solvent B (0.01% formic acid in acetonitrile, v/v) was used in gradient mode for separation. The elution gradient was described below: 0 min, 5 % B; 1.5 min, 5 % B; 9 min, 70 % B; 10 min, 70 % B; 10.1 min, 5 % B; 15 min, 5 % B. While the injection volume, flow rate and mobile phase was same to that used for the phytohormone analysis as described above, the compounds were detected in the ESI negative mode. Molecular ions ([M-H]⁻) with m/z 209.1183 (JA) and 137.02442 (SA) were fragmented, and relevant unique daughter ions 59.0139 (JA), and 93.0345 (SA) were recorded for quantification. The concentration of phytohormones was quantified using a calibration equation obtained by linear regression from five calibration points for each analysis.

Text S8. The parameters of UHPLC-MS/MS for determining taproot metabolites

The UHPLC-MS/MS system mobile phase A was 0.1% formic acid in water, and the mobile phase B was 0.1% formic acid in acetonitrile. The elution gradient was set as follows: 0 min, 5 % B; 1.5 min, 5% B; 10 min, 100 % B; 11min 100%B; 11.5 min, 5 % B; 14 min, 5 % B. The flow rate was 0.35 mL/min. To evaluate the stability of the analytical system, QC samples were collected after every 6 samples. The conditions of ESI were: sheath gas pressure, 35 arbitrary units; aux gas flow, 15 arbitrary units; sweep gas flow, 0 arbitrary units; capillary temperature, 320 °C; aux gas heater temperature, 350 °C. Spray voltage was 3.5 kV for ESI (positive) and -3.0 kV for ESI (negative). Compound Discoverer 3.1 software coupled with the mzCloud and Chem Spider libraries were used to process the raw data files.⁸ Moreover, partial least-squares discriminant analysis (PLS-DA) and biological pathway analysis were performed based on UHPLC-MS/MS data using MetaboAnalyst 5.0 online tool (<https://www.metaboanalyst.ca/>) to detect differential metabolites and disturbed metabolic pathways. The variable importance in projection (VIP) score was used to rank the metabolites based on their importance to the entire model. Metabolite satisfied $VIP > 1$ (based on PLS-DA analysis) and $P < 0.05$ was considered as differential metabolites between the control groups and treatments (Si QDs exposure and SS exposure). The selected differential metabolites were analysed for further KEGG pathway analysis. Disturbed metabolic pathways were considered important if they fulfilled the following criteria: i) the ratio of the number of metabolites hits to the total metabolites of the pathway is greater than one; ii) $P < 0.05$; iii) impact rates of the route > 0.1 .⁹

Text S9. Analysis of rhizosphere soil microbiome

The total soil DNA was extracted from 0.3g fresh radish rhizosphere soil using the DNeasy PowerSoil Kit (QIAGEN, Inc., Netherlands) following the manufacturer's instructions. The quantity and quality of extracted DNA were assessed using a NanoDrop ND-1000 spectrophotometer (Thermo Fisher Scientific, USA) and agarose

gel electrophoresis, respectively. PCR amplification of V3-V4 variable regions of the bacterial 16S rRNA genes was performed using the forward primer 338F (5'-ACTCCTACGGGAGGCAGCA-3') and the reverse primer 806R (5'-GGACTACHVGGGTWTCTAAT-3'). PCR amplicons were purified with Agencourt AMPure Beads (Beckman Coulter, Indianapolis, IN) and quantified using the PicoGreen dsDNA Assay Kit (Invitrogen, Carlsbad, CA, USA). Afterward, purified amplicons were pooled in equal amounts, and sequenced using Illumina MiSeq platform (Shanghai Personal Biotechnology Co., Ltd. Shanghai, China). Sequence data were demultiplexed, filtered for quality, and assigned to exact amplicon sequence variants (ASVs) using the QIIME2 (version 2019.7).¹⁰

Table S1. Typical sensitivity, detection limits and R² for Si element detection by ICP-MS.

Parameter	Value
m/z	28
Linearity range (mg/L)/R ²	0-40/0.9997
Linearity equation	y = 1509.200x+1308.400
detection limit (ug/L)	171
Spike recovery	101.6%
Bush branches and leaves (GBW07602):	5800 ± 400
Standard value (µg/g)	
Bush branches and leaves (GBW07602):	5442 ± 201.3
ICP-MS measured value (µg/g, n = 3)	

Table S2. Primer sets list for this study.

Gene	Primer	Sequence (5' to 3')	Reference	
<i>RsPAL2</i>	Forward	AACAGTATTCTTCACAGTCT	11	
	Reverse	GCTTGGATTACGGATTCA		
<i>RsC4H</i>	Forward	GATTGGTAGGTTGGTTCA		
	Reverse	TGGCTTCATTACGATTGT		
<i>RsF5H</i>	Forward	CCATTAGTTCATCCACCAT		
	Reverse	TTCGTCAAGATTCTACAGG		
<i>RsCOMT</i>	Forward	CCTTGTAGCAGTTCTTCA		
	Reverse	GATGTTGGTGGTGGTATT		
<i>RsCAD3</i>	Forward	GACAATGGTGACAATGATG		
	Reverse	GGAACGACAGGATAATAGG		
<i>RsCCoAOMT1</i>	Forward	GCAACGAAGACATCTACTA		
	Reverse	GATTCTGGTTCTCTTGGATA		
<i>RsPRI</i>	Forward	GCAGACTCGTACACTCCGGTGGGC		
	Reverse	GCCTTCTCGCTAACCCAAAGGTTC		
<i>RsPR2</i>	Forward	GTACGCTCTGTTCAAACCGACCC		
	Reverse	TTCCAACGATCCTCCGCCTGA		
<i>RsPR3</i>	Forward	TCTTTGGTCAGACTTCCCACGAG		12
	Reverse	GATGGCTCTTCCCACTGTCCGTA		
<i>RsLOX</i>	Forward	GACGATACCAGACTACCCATTT		
	Reverse	CTTCACTTCACTCCACCATTC		
<i>RsMYC2</i>	Forward	TTATCATCGCATCCCAAC		
	Reverse	CGCTATCGCTTACATCAA		
<i>RsAOC3</i>	Forward	GTTCCCTCGCCGTCACCTGTGG	13	
	Reverse	GTAACCGCCGTCCCAGTAAGC		
<i>Actin2/7</i>	Forward	GCATCACACTTTCTACAAC	12	
	Reverse	CCTGGATAGCAACATACAT		

Table S3. Two-way ANOVA table summarizing the interactive effects of Si treatment and herbivore treatment with white grubs on radish plant growth, antioxidant enzymes activity, oxidative stress and plant defense traits. The test results are shown with the test statistic F-value and significance levels ($***P < 0.001$, $** P < 0.01$, $* P < 0.05$ and $^{NS} P > 0.05$).

Plant traits	Si treatment	Herbivore	Si treatment × Herbivore
Shoot biomass	2.8 ^{NS}	3.9 ^{NS}	0.3 ^{NS}
Taproot biomass	5.0 ^{***}	8.9 ^{***}	0.4 ^{NS}
Leaf chlorophyll	65.8 ^{***}	23.3 ^{***}	2.1 ^{NS}
Leaf Pn	20.7 ^{***}	6.8 [*]	0.9 ^{NS}
Taproot SOD	11.7 ^{***}	133.8 ^{***}	5.5 ^{**}
Taproot POD	8.8 ^{***}	0.1 ^{NS}	0.7 ^{NS}
Taproot CAT	2.2 ^{NS}	18.1 ^{***}	1.8 ^{NS}
Taproot MDA	18.3 ^{***}	58.5 ^{***}	6.3 ^{**}
Taproot Si	12.8 ^{***}	101.1 ^{***}	0.1 ^{NS}
Taproot lignin	35.2 ^{***}	23.4 ^{***}	3.5 [*]
Taproot JA	5.5 [*]	26.1 ^{***}	1.3 ^{NS}
Taproot SA	15.2 ^{***}	181.5 ^{***}	1.8 ^{NS}
Taproot aucubin	0.3 ^{NS}	55.5 ^{***}	4.4 [*]
Taproot catalpol	4.3 [*]	42.4 ^{***}	4.5 [*]
Taproot gluconasturtiin	21.3 ^{***}	3.6 ^{NS}	1.5 ^{NS}

Table S4. Relative abundances of top 10 bacterial phyla in rhizosphere soils in response to treatments (CK, Si QDs, sodium silicate (SS), and imidacloprid (IM)).

Phylum	CK	Si QDs	SS	IM
<i>Proteobacteria</i>	44.91±2.58 a	44.22±0.98 a	41.88±5.19 a	46.72±1.38 a
<i>Actinobacteria</i>	10.66±0.53 a	9.66±1.69 a	13.59±3.87 a	10.54±0.61 a
<i>Cyanobacteria</i>	9.49±1.96 a	8.77±0.2 a	6.72±1.19 a	10.25±1.17 a
<i>Chloroflexi</i>	7.56±0.67 a	7.51±0.44 a	10.49±3.61 a	7.5±0.87 a
<i>Bacteroidetes</i>	7.56±0.42 a	7.54±0.65 a	5.79±1.84 a	6.08±0.54 a
<i>Acidobacteria</i>	4.19±0.37 b	6.19±0.42 a	5.22±0.57 ab	5.23±0.2 ab
<i>Firmicutes</i>	5.17±0.36 a	3.95±0.14 a	6.16±0.77 a	3.41±1.12 a
<i>Gemmatimonadetes</i>	4.14±0.25 a	4.25±0.54 a	4.78±0.49 a	4.58±0.43 a
<i>Patescibacteria</i>	2.5±0.05 a	3.36±0.3 a	2.15±0.25 a	3.07±0.43 a
<i>Nitrospirae</i>	0.85±0.1 b	1.3±0.06 a	1.12±0.09 ab	0.8±0.1 b
<i>Others</i>	2.97±0.28 ab	3.25±0.4 a	2.11±0.16 ab	1.83±0.15 b

Data were means ± SE (n = 3). Different lowercase letters indicated significant differences among treatments (Tukey's HSD test, $P < 0.05$).

Table S5. Relative abundances of top 20 bacterial genera in rhizosphere soils in response to different treatments (CK, Si QDs, sodium silicate (SS), and imidacloprid (IM)).

Genus	CK	Si QDs	SS	IM
<i>MND1</i>	1.86 ± 0.23 a	1.39 ± 0.12 a	1.96 ± 0.18 a	1.71 ± 0.09 a
<i>Pseudomonas</i>	1.2 ± 0.33 a	1.08 ± 0.06 a	1.39 ± 0.28 a	1.29 ± 0.43 a
<i>Blrii41</i>	2.63 ± 0.64 a	2.00 ± 0.47 a	1.5 ± 0.23 a	1.93 ± 0.55 a
<i>Methylophaga</i>	1.68 ± 0.21 a	0.27 ± 0.02 b	0.55 ± 0.24 b	0.81 ± 0.09 b
<i>HOC36</i>	1.35 ± 0.66 a	0.59 ± 0.22 a	0.85 ± 0.4 a	0.56 ± 0.09 a
<i>Chloronema</i>	1.35 ± 0.6 a	0.46 ± 0.11 a	0.74 ± 0.39 a	0.51 ± 0.06 a
<i>Haliangium</i>	1.83 ± 0.24 a	1.72 ± 0.13 a	2.25 ± 0.42 a	3.84 ± 0.74 a
<i>Saccharimonadales</i>	1.21 ± 0.05 a	1.43 ± 0.08 a	1.27 ± 0.15 a	2.04 ± 0.35 a
<i>Arenimonas</i>	1.24 ± 0.2 a	1.04 ± 0.14 a	0.8 ± 0.12 a	1.53 ± 0.42 a
<i>TRA3-20</i>	1.67 ± 0.07 a	1.72 ± 0.13 a	1.38 ± 0.19 a	1.91 ± 0.12 a
<i>Tychonema_CCAP_1459-11B</i>	1.3 ± 0.46 a	1.51 ± 0.19 a	0.64 ± 0.21 a	1.56 ± 0.36 a
<i>Hydrogenophaga</i>	0.73 ± 0.13 a	1.35 ± 0.26 a	0.72 ± 0.07 a	0.62 ± 0.06 a
<i>Ramlibacter</i>	1.43 ± 0.13 b	2.11 ± 0.07 a	1.47 ± 0.12 b	1.45 ± 0.1 b
<i>Subgroup_10</i>	0.77 ± 0.04 a	1.39 ± 0.15 a	0.73 ± 0.09 a	0.73 ± 0.09 a
<i>Nitrospira</i>	0.84 ± 0.09 b	1.3 ± 0.06 a	1.12 ± 0.09 ab	0.79 ± 0.1 b
<i>A4b</i>	0.9 ± 0.21 a	1.15 ± 0.09 a	0.99 ± 0.24 a	0.84 ± 0.22 a
<i>Sphingomonas</i>	0.68 ± 0.04 a	1.02 ± 0.16 a	0.77 ± 0.19 a	0.95 ± 0.18 a
<i>Subgroup_6</i>	1.92 ± 0.2 a	2.48 ± 0.1 a	2.45 ± 0.24 a	2.41 ± 0.24 a
<i>Ellin6067</i>	0.95 ± 0.07 a	1.16 ± 0.04 a	1.27 ± 0.22 a	1.29 ± 0.14 a
<i>FFCH7168</i>	0.57 ± 0.05 a	0.74 ± 0.14 a	0.82 ± 0.33 a	0.86 ± 0.19 a

Data were means ± SE (n = 3). Different lowercase letters indicated significant differences among treatments (Tukey's HSD test, $P < 0.05$).

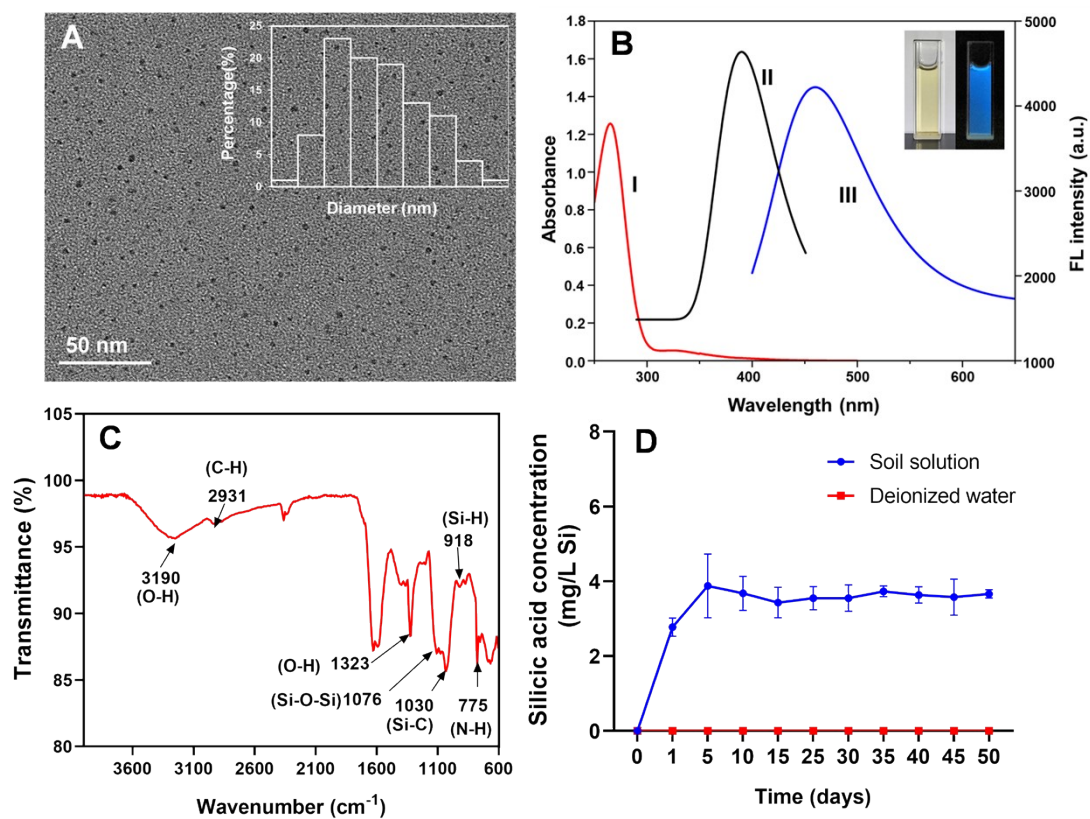


Fig. S1 Characterization of Si QDs: TEM image and diameter distribution (A); UV-vis absorption spectrum (I), excitation spectrum (II), fluorescence emission spectrum (III) (B); FT-IR spectrum (C); The dissolution rate of Si QDs (50 mg/L) in deionized water and soil solution during 50 days (D).

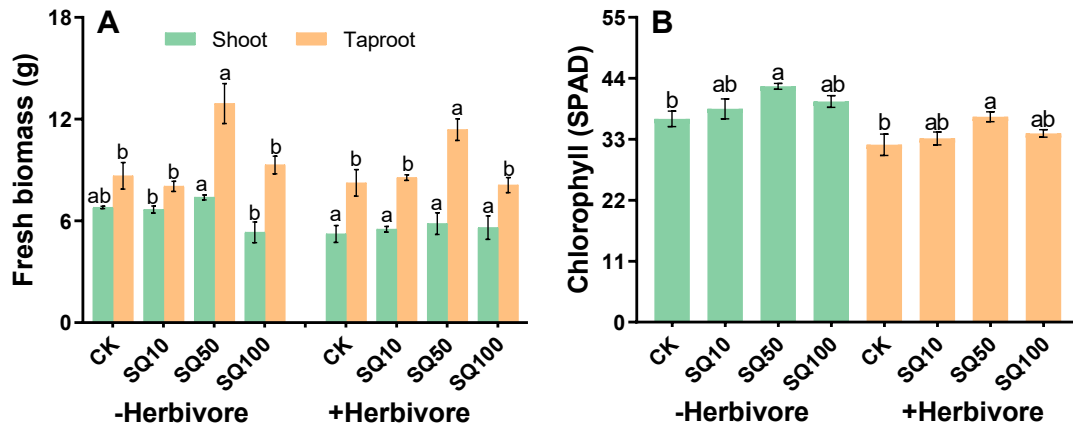


Fig. S2 Preliminary experiment for testing the dose-dependent effect of Si QDs on shoot (green bars) and taproot (orange bars) fresh biomass (A) and leaf chlorophyll content (B) of cherry radish without (-Herbivore) and with (+Herbivore) the presence of white grubs. Soil additions of Si QDs were at the dose of 0, 10, 50 and 100 mg/kg (CK, SQ10, SQ50, SQ100). Data are means \pm SE ($n = 3$). Different letters represent significant differences among different treatments in the absence and presence of white grubs, respectively (Tukey's HSD test, $P < 0.05$).



Fig. S3 Photos of the radish growth without (-Herbivore) and with (+Herbivore) the presence of white grubs exposed to Si quantum dots (Si QDs), sodium silicate (SS), and imidacloprid (IM).

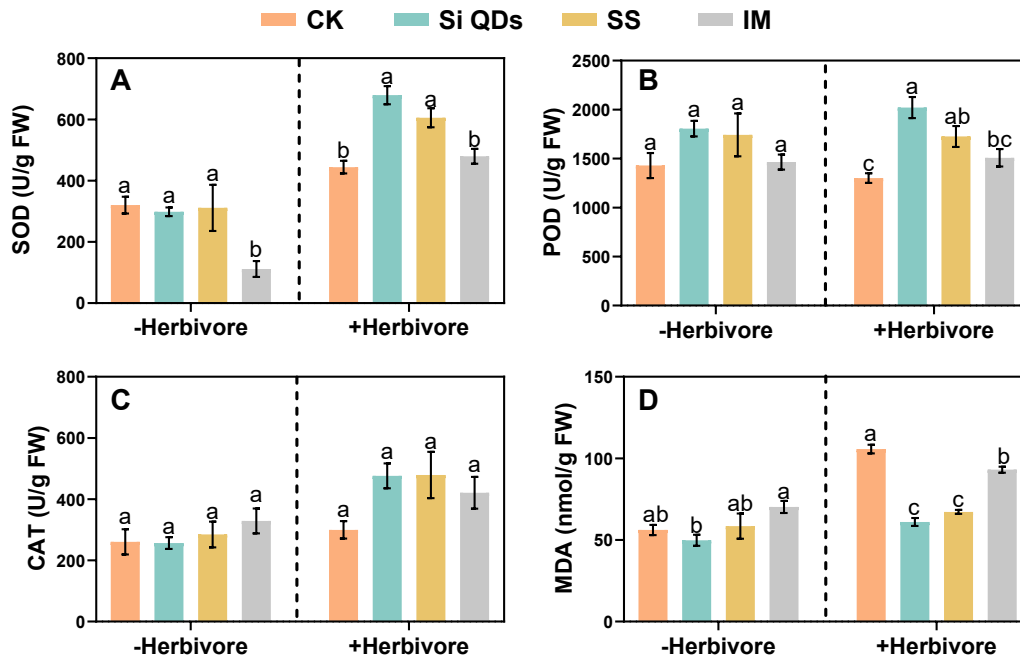


Fig. S4 Taproot SOD (A), POD (B), CAT(C), MDA (D) of radish without (-Herbivore) and with (+Herbivore) the presence of white grubs exposed to Si quantum dots (Si QDs), sodium silicate (SS), and imidacloprid (IM). Data are means \pm SE ($n = 5$). Different letters represent significant differences among treatments in the absence and presence of white grubs, respectively (Tukey's HSD test, $P < 0.05$).

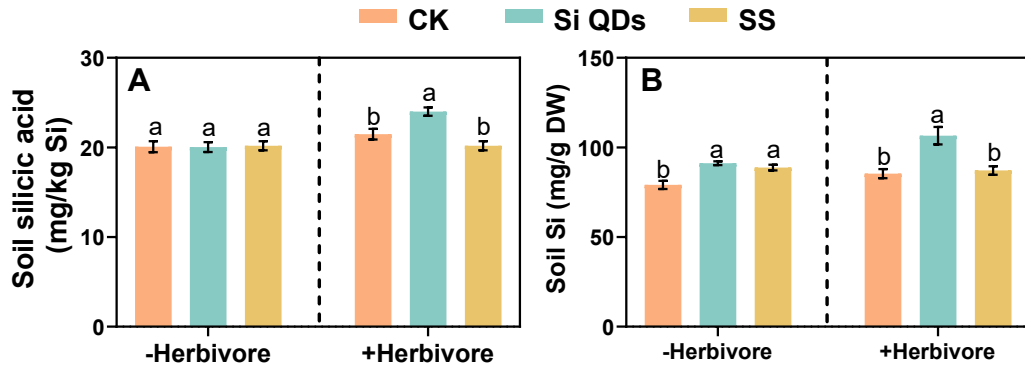


Fig. S5 Effect of soil addition with Si quantum dots (Si QDs), sodium silicate (SS), imidacloprid (IM) on soil silicic acid content (A) and soil Si content (B) without (-Herbivore) and with (+Herbivore) the presence of white grubs. Data are means \pm SE (n = 5). Different letters represent significant differences among treatments in the absence and presence of white grubs, respectively (Tukey's HSD test, $P < 0.05$).

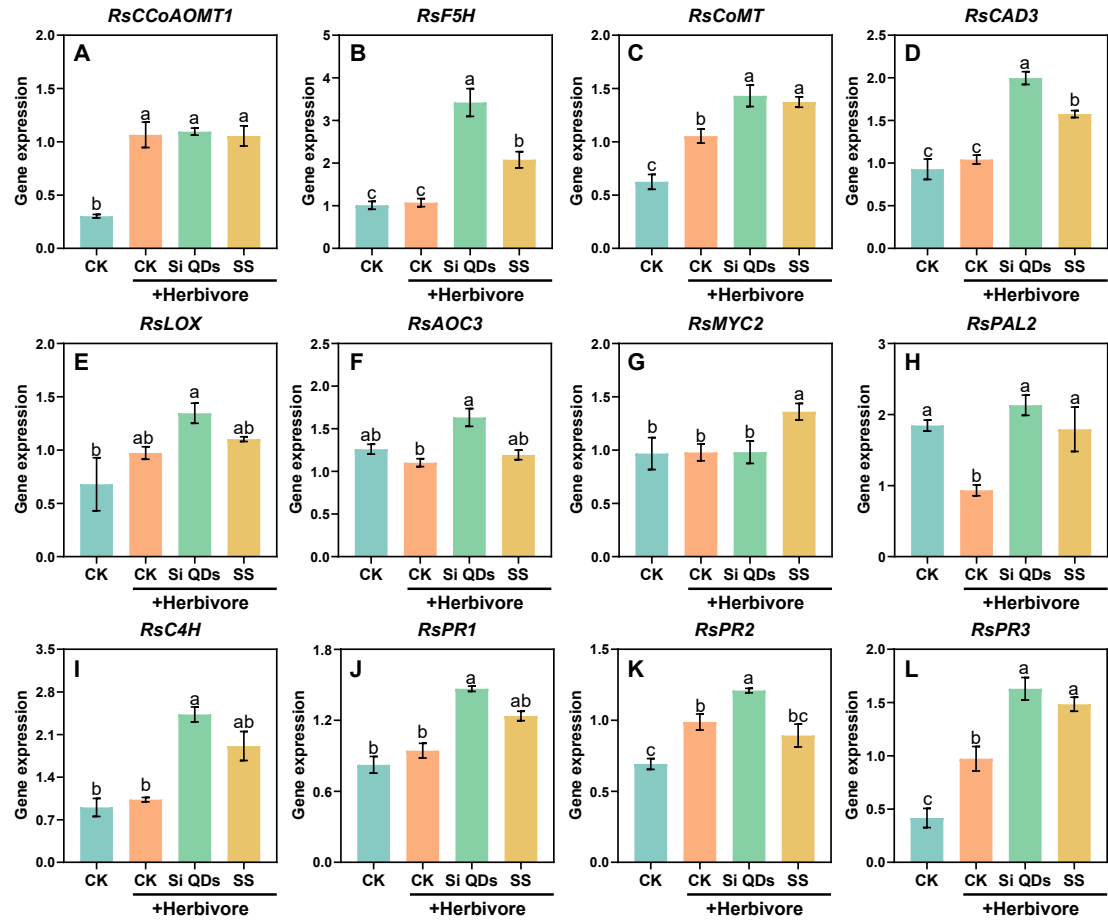


Figure S6. The relative expression of the lignin biosynthesis genes (A-D), JA biosynthesis (E, F) and JA-dependent defense response genes (G), SA biosynthesis (H, I) and the marker genes of SA-dependent systemic acquired resistance (J-L) in radish root. Data shown are means \pm SE ($n = 3$). Different letters indicate significant differences among treatments (Tukey's HSD test, $P < 0.05$).

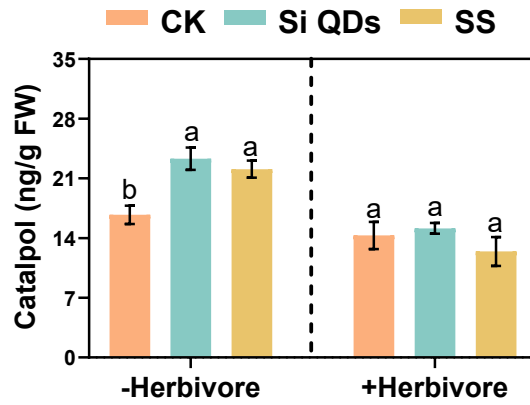


Fig. S7 Effect of soil addition with Si quantum dots (Si QDs) and sodium silicate (SS) on radish taproot catalpol content without (-Herbivore) and with (+Herbivore) the presence of white grubs. Data are means \pm SE ($n = 5$). Different letters represent significant differences among treatments in the absence and presence of white grubs, respectively (Tukey's HSD test, $P < 0.05$).

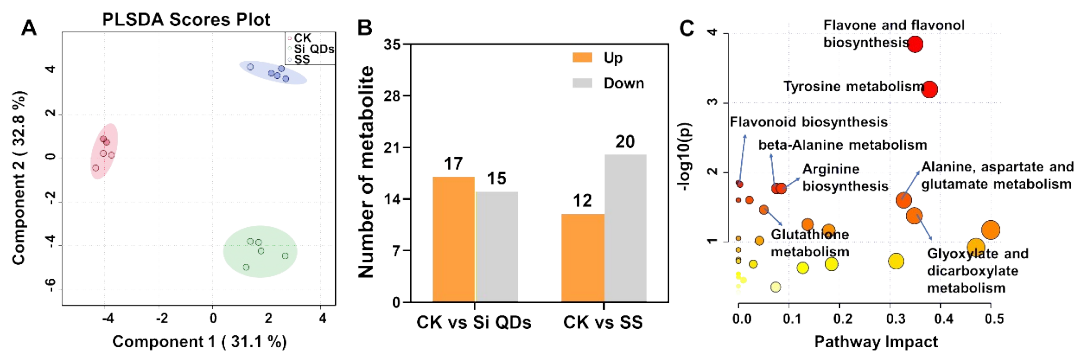


Fig. S8 PLS-DA plots of metabolic features of herbivore-stressed radish taproot exposed to Si treatments (A). Numbers of up-regulated and down-regulated differential metabolites between CK group and other group (Si QDs and sodium silicate (SS), B). Summary of the pathway analysis of radish taproot metabolites in response to herbivory with the MetaboAnalyst 5.0 (C).

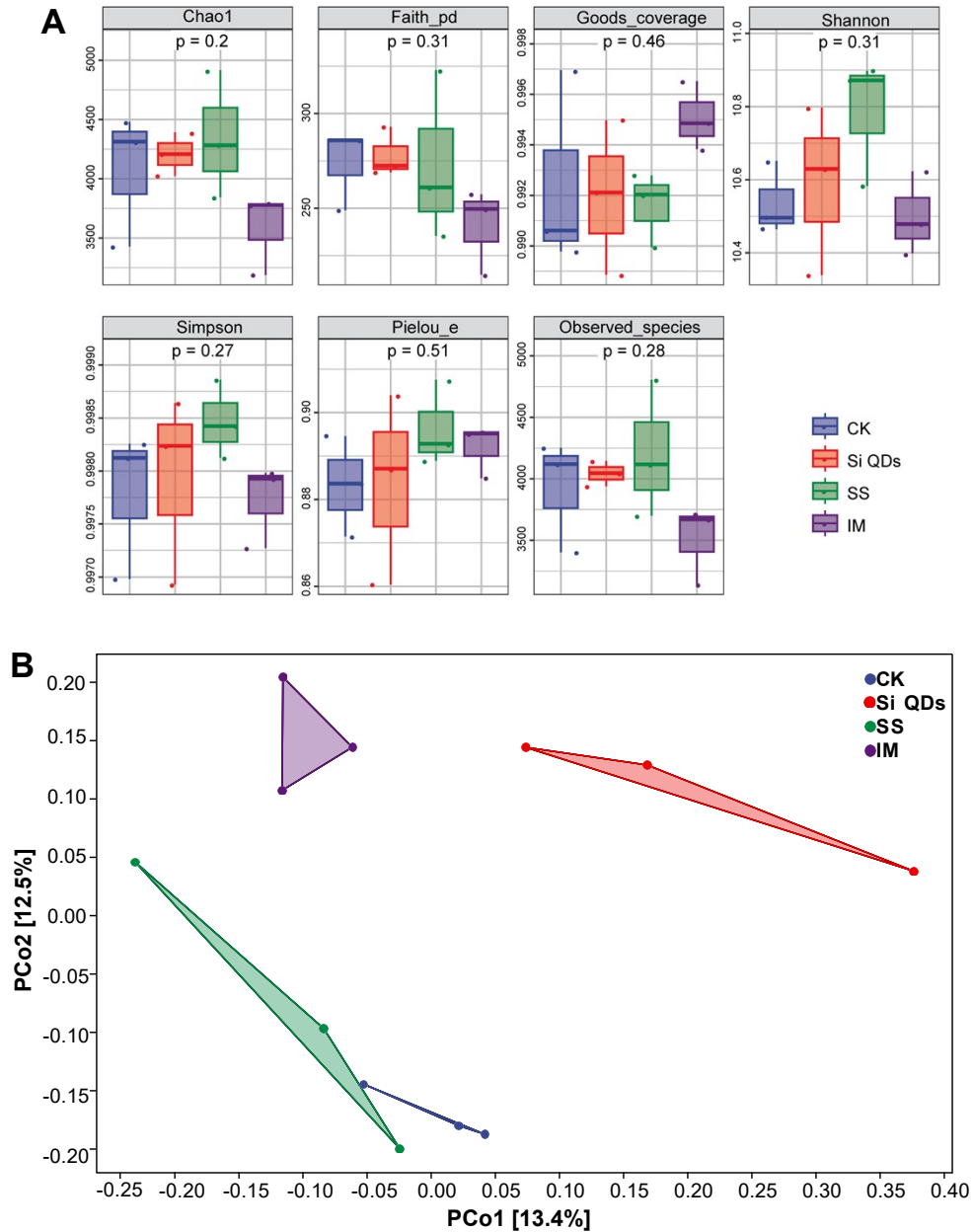


Fig. S9 Microbial alpha diversity indexes (A) and principal coordinate analysis (PCoA) diagrams (B) of radish soil microorganism in the presence of white grubs in response to different treatments (CK, Si quantum dots (Si QDs), sodium silicate (SS), and imidacloprid (IM)).

References

1. M. Na, Y. Chen, Y. Han, S. Ma, J. Liu and X. Chen, Determination of potassium ferrocyanide in table salt and salted food using a water-soluble fluorescent silicon quantum dots, *Food Chem.*, 2019, **288**, 248-255.
2. H. Kang, W. Elmer, Y. Shen, N. Zuverza-Mena, C. Ma, P. Botella, J. C. White and C. L. Haynes, Silica nanoparticle dissolution rate controls the suppression of *Fusarium wilt* of watermelon (*Citrullus lanatus*), *Environ. Sci. Technol.*, 2021, **55**, 13513-13522.
3. W. Ma, L. Yue, F. Chen, H. Ji, N. Fan, M. Liu, Z. Xiao and Z. Wang, Silica nanomaterials and earthworms synergistically regulate maize root metabolite profiles via promoting soil Si bioavailability, *Environ. Sci.: Nano*, 2021, **8**, 3865-3878.
4. N. Ma, C. Hu, L. Wan, Q. Hu, J. Xiong and C. Zhang, Strigolactones improve plant growth, photosynthesis, and alleviate oxidative stress under salinity in rapeseed (*Brassica napus* L.) by regulating gene expression, *Front. Plant Sci.*, 2017, **8**, 1671.
5. X. Luo, X. Cao, C. Wang, L. Yue, X. Chen, H. Yang, X. Le, X. Zhao, F. Wu, Z. Wang and B. Xing, Nitrogen-doped carbon dots alleviate the damage from tomato bacterial wilt syndrome: systemic acquired resistance activation and reactive oxygen species scavenging, *Environ. Sci.: Nano*, 2021, **8**, 3806-3819.
6. Z. Y. Wang, W. Q. Zhu, F. R. Chen, L. Yue, Y. Ding, H. Xu, S. Rasmann and Z. G. Xiao, Nanosilicon enhances maize resistance against oriental armyworm (*Mythimna separata*) by activating the biosynthesis of chemical defenses, *Sci. Total Environ.*, 2021, 778.
7. Z. Xiao, N. Fan, W. Zhu, H.-L. Qian, X.-P. Yan, Z. Wang and S. Rasmann, Silicon nanodots increase plant resistance against herbivores by simultaneously activating physical and chemical defenses, *ACS Nano*, 2023, **17**, 3107-3118.
8. Z. Wang, J. Tang, L. Zhu, Y. Feng, L. Yue, C. Wang, Z. Xiao and F. Chen, Nanomaterial-induced modulation of hormonal pathways enhances plant cell growth, *Environ. Sci.: Nano*, 2022, **9**, 1578-1590.
9. A. I. Tristan, A. C. Abreu, L. M. Aguilera-Saez, A. Pena, A. Conesa-Bueno and I. Fernandez, Evaluation of ORAC, IR and NMR metabolomics for predicting ripening stage and variety in melon (*Cucumis melo* L.), *Food Chem.*, 2022, **372**,

131263.

10. Z. Xiao, N. Fan, X. Wang, H. Ji, L. Yue, F. He and Z. Wang, Earthworms drive the effect of La₂O₃ nanoparticles on radish taproot metabolite profiles and rhizosphere microbial communities, *Environ. Sci. Technol.*, 2022, **56**, 17385-17395.
11. H. Feng, L. Xu, Y. Wang, M. Tang, X. Zhu, W. Zhang, X. Sun, S. Nie, E. M. m. Muleke and L. Liu, Identification of critical genes associated with lignin biosynthesis in radish (*Raphanus sativus* L.) by de novo transcriptome sequencing, *Mol. Genet. Genomics*, 2017, **292**, 1151-1163.
12. K. Yoshida, M. Uefune, R. Ozawa, H. Abe, Y. Okemoto, K. Yoneya and J. Takabayashi, Effects of prohydrojasmon on the number of infesting herbivores and biomass of field-grown Japanese radish plants, *Fron. Plant Sci.*, 2021, **12**, 695701.
13. A. Tkachenko, I. Dodueva, V. Tvorogova, A. Predeus, O. Pravdina, K. Kuznetsova and L. Lutova, Transcriptomic analysis of radish (*Raphanus sativus* L.) spontaneous tumor, *Plants*, 2021, **10**, 919.